

Novel Mechanism of Activation of NADPH Oxidase 5 CALCIUM SENSITIZATION VIA PHOSPHORYLATION*

Received for publication, September 20, 2006, and in revised form, December 11, 2006. Published, JBC Papers in Press, December 12, 2006, DOI 10.1074/jbc.M608966200

Davin Jagnandan[‡], Jarrod E. Church[‡], Botond Banfi[§], Dennis J. Stuehr[¶], Mario B. Marrero[‡], and David J. R. Fulton^{‡1}

From the [‡]Department of Pharmacology and the Vascular Biology Center, Medical College of Georgia, Augusta, Georgia 30912-2500, the [§]Department of Anatomy, University of Iowa College of Medicine, Coralville, Iowa 52241, and the [¶]Departments of Immunology and Pathobiology, Lerner Research Institute, Cleveland Clinic Foundation, Cleveland, Ohio 44195

In contrast to other Nox isoforms, the activity of Nox5 does not require the presence of accessory proteins and is entirely dependent on the elevation of intracellular calcium. Previous studies have shown that the EC_{50} of Nox5 for calcium is relatively high and raises the question of whether Nox5 can be sufficiently activated in cells that do not experience extreme elevations of intracellular calcium. In the current study, we have identified a novel mechanism governing the activity of Nox5. Exposure of cells expressing Nox5 to phorbol 12-myristate 13-acetate (PMA) resulted in a slow and sustained increase in ROS, which was markedly different from the rapid response to ionomycin. PMA greatly potentiated the activity of Nox5 in response to low concentrations of ionomycin. The ability of PMA to increase Nox5 activity was abolished by calcium chelation and was a direct effect on enzyme activity, since PMA increased the calcium sensitivity of Nox5 in a cell-free assay. PMA stimulated the time-dependent phosphorylation of Nox5 on Thr⁴⁹⁴ and Ser⁴⁹⁸. Mutation of these residues to alanine abolished both PMA-dependent phosphorylation and calcium sensitization. Conversely, mutation of Thr⁴⁹⁴ and Ser⁴⁹⁸ to glutamic acid produced a gain of function mutant that had increased activity at low concentrations of ionomycin. Within the cell, Nox5 was detected in detergent-resistant microdomains of the endoplasmic reticulum. In summary, the phosphorylation of Nox5 at key residues facilitates enzyme activation at lower levels of intracellular calcium and may provide an avenue for enzyme activation in response to a greater variety of extracellular stimuli.

The NADPH oxidases or Noxs define a unique family of enzymes that exist to synthesize reactive oxygen species (ROS)² (1). Currently, five distinct Noxs have been identified and are numbered Nox1 to -5. Of these, Nox2 is the best characterized

and is expressed primarily by cells of the immune system, including neutrophils and macrophages. Mutation of Nox2 or targeted disruption in mice results in impaired host defense (2). The biological functions of Noxs that are expressed in cells outside of the immune system are emerging but remain somewhat enigmatic. However, the considerable diversity that exists in the location, the capacity, and the mechanisms by which these enzymes are activated suggests that they have indeed evolved distinct functional roles.

The mechanisms that control the synthesis of ROS by the various Nox isoforms are remarkable in their complexity. Nox2 is a transmembrane glycoprotein that is activated by the coordinated assembly of at least five distinct subunits. In unstimulated cells, Nox2 is bound to the protein p22^{phox}, and upon activation, the coalescence of p67^{phox}, p47^{phox}, p40^{phox}, and Rac yields a functional, superoxide-generating oxidase (1, 3). Nox1 is also bound to p22^{phox} and is activated by the subunits NOXA1 and NOXO1, which are functionally related to p67^{phox} and p47^{phox}, respectively (4, 5). The activity of Nox3 can be regulated by p22^{phox}, p67^{phox}, p47^{phox}/p67^{phox}, or NOXO1, but compared with Nox2, it is less discriminating in which subunits are required for full activation (6, 7). The activity of Nox4 is largely constitutive, but it is at least in part dependent on the co-association of p22^{phox} for full activity (8, 9). In contrast, Nox5 is a calcium-dependent enzyme and does not depend on the assembly of other proteins, including p22^{phox}, for its activity (8, 10, 11).

Nox5, like the other Nox isoforms, is a membrane-bound oxidase that spans the membrane six times (10). However, Nox5 is distinct in that its N terminus contains four EF hands that bind calcium and regulate its activity. In a cell-free system, the activity of membrane-bound Nox5 was shown to be entirely dependent on calcium. The addition of cytosol or cytosolic proteins that can activate Nox2 in cell-free assays did not increase the activity of Nox5 (11). The amino terminus of Nox5 operates in a manner analogous to calmodulin, whereby calcium binding initiates a conformational change in the enzyme. This permits the interaction of the N terminus of Nox5 with a yet to be identified C-terminal domain, which then facilitates electron delivery and the production of reactive oxygen species (11). In cell-free assays, the EC_{50} for calcium was determined to be $\sim 1 \mu\text{M}$, which is relatively high and unlikely to be achieved in most cells outside of extraordinary circumstances (11).

In the context of the above model of Nox5 activation, the current study identifies a novel mechanism regulating the activ-

* This work was supported by National Institutes of Health Grant HL74279 (to D. F.). The costs of publication of this article were defrayed in part by the payment of page charges. This article must therefore be hereby marked "advertisement" in accordance with 18 U.S.C. Section 1734 solely to indicate this fact.

¹ To whom correspondence should be addressed: Vascular Biology Center, Medical College of Georgia, 1459 Laney Walker Blvd., Augusta, GA 30912-2500. Tel.: 706-721-1946; Fax: 706-721-9799; E-mail: dfulton@mccg.edu.

² The abbreviations used are: ROS, reactive oxygen species; RLU, relative light units; PMA, phorbol 12-myristate 13-acetate; WT, wild type; GFP, green fluorescent protein; RFP, red fluorescent protein; EGFP, enhanced green fluorescent protein; PKC, protein kinase C; MOPS, 4-morpholinopropane-sulfonic acid; CIP, calf intestinal phosphatase; DPI, diphenyleioidonium; SOD, superoxide dismutase.

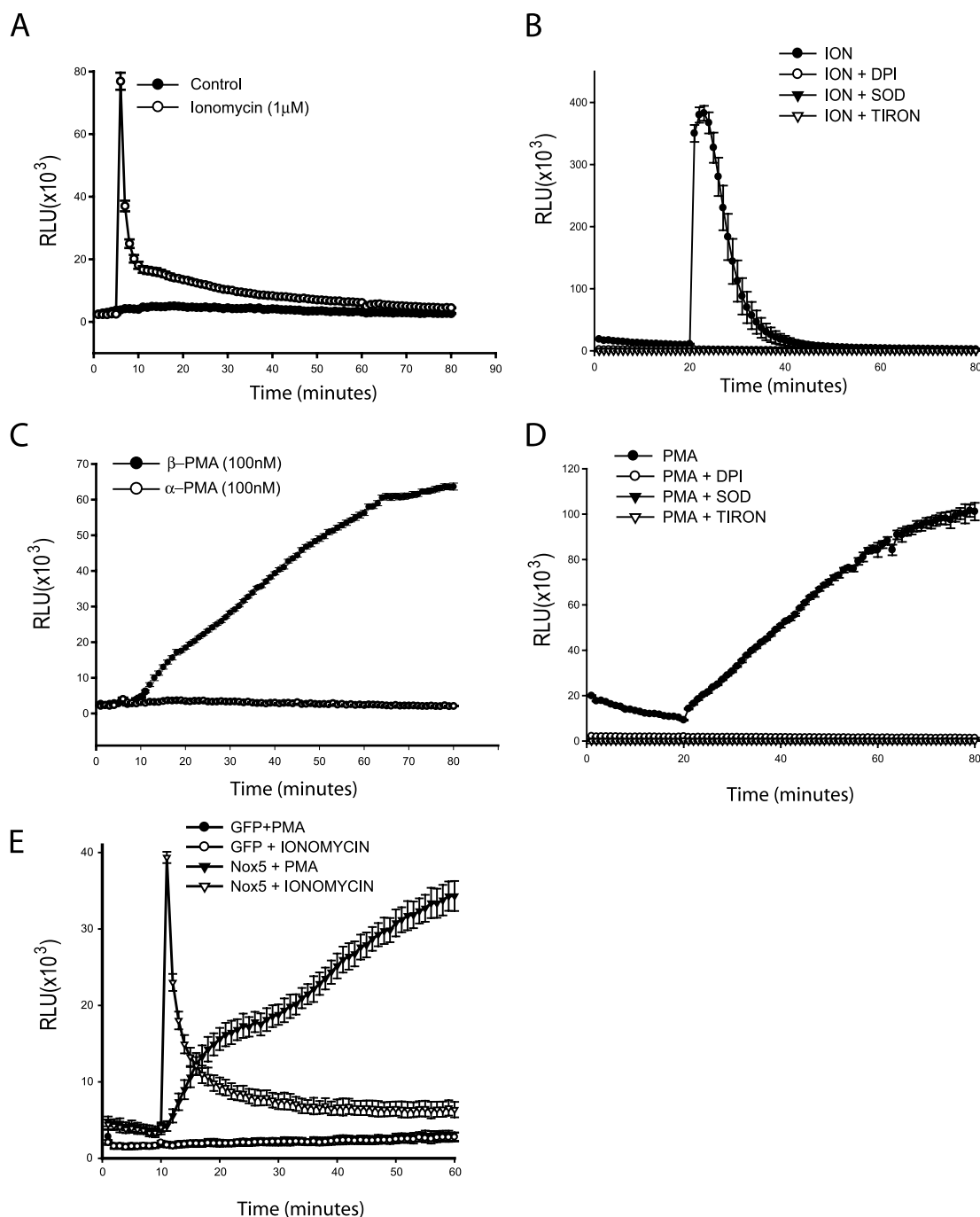


FIGURE 1. Activation of Nox5 via distinct mechanisms. COS-7 cells were transfected with Nox5 or GFP (control) cDNA and stimulated with ionomycin (1 μ M, open symbols) or vehicle (Me₂SO; solid symbols) (A) in the presence or absence of the flavoprotein inhibitor, DPI (10 μ M), or the superoxide scavengers, SOD (100 units/ml) and 1,2-dihydroxybenzene-3,5-disulfonate (TIRON; 5 mM) (B). C, Nox5-transfected cells were stimulated with α (open symbols) or β (solid symbols) PMA (100 nM) in the presence or absence of DPI, SOD, or TIRON (D). E, cells were transfected with Nox5 cDNA (triangles) or control plasmid GFP (circles) and stimulated with ionomycin (1 μ M; open symbols) or β -PMA (100 nM; solid symbols). Production of ROS was determined via chemiluminescence and expressed as relative light units (RLU $\times 10^3$, means \pm S.E., $n = 4$). Results are representative of more than three independent experiments.

ity of Nox5 and provides a more physiological context for enzyme activation at lower levels of intracellular calcium.

EXPERIMENTAL PROCEDURES

Cell Culture and Transfection—COS-7 cells were cultured in Dulbecco's modified Eagle's medium (Invitrogen) containing L-glutamine, penicillin, streptomycin, and 10% (v/v) fetal bovine serum. Cells were transfected with LipofectamineTM 2000 according to the manufacturer's instructions (Invitrogen).

Measurement of Reactive Oxygen Species—COS-7 cells were transfected with cDNAs encoding Nox5 or control plasmids (GFP, RFP, or LacZ), and 24 h later, cells were replated into white tissue culture-treated 96-well plates (ThermoLab-systems) at a density of $\sim 5 \times 10^4$ cells/well. The cells were incubated at 37 $^{\circ}$ C in phenol-free Dulbecco's modified Eagle's medium (Sigma) containing a 400 μ M concentration of the luminol analogue L-012 (Wako) for a minimum of 20 min prior to the addition of agonists (12). Luminescence was quantified

Activation of Nox5 via Phosphorylation

over time using a Lumistar Galaxy (BMG) luminometer. The specificity of L-012 for reactive oxygen species was confirmed by transfecting cells with a control plasmid, such as GFP or LacZ or by co-incubation of a superoxide scavenger, such as TIRON (5 mM). Both of these interventions yielded virtually undetectable levels of luminescence under control or PMA- or ionomycin-stimulated conditions. Thus, the relative light units (RLU) quantified from the luminescence of L-012 are reflective of changes in the activity of Nox5. In additional experiments, the activity of Nox5 was also verified using a commercially available kit that is specific for superoxide (Diogenes; National Diagnostics).

DNA Constructs—Nox5 β (accession number AF325189) was subcloned into a modified pcDNA3 containing an N-terminal HA epitope, and sequence was verified by the Genomics Core Facility of the Medical College of Georgia. GFP- and RFP-tagged Nox5 were generated similarly and subcloned into pcDNA3 expression plasmids as previously described (13). endoplasmic reticulum-RFP (DSRED) and tubulin-EGFP were obtained from Clontech. RFP-nucleus, Golgi-RFP, MITO-RFP, and PM-RFP have been described elsewhere (13, 14). A phospho-null Nox5 construct encoding the S486A, S490A, T494A, and S498A mutations was generated by PCR using WT Nox5 cDNA as a template and the following primers: forward, 5'-GCT AAG AGG CTG GCC AGG AGT GTG GCA ATG AGA AAG GCT CAA AGG TCG TCC AAG GGC-3'; reverse, 5'-AGC CTT TCT CAT TGC CAC ACT CCT GGC CAG CCT CTT AGC ACC ACG GCC CAG TGG GTC-3'. Individual mutants were generated with the following primers: S486A (5'-gaccactgggccgtggGctaagaggctgtcgag-3'), S490A (5'-ggttctaagaggctgGcCaggagtgtgacaatgag-3'), T494A (5'-gctgtcaggagtgtgGcaatgagaagaggtcaag-3'), and S498A (5'-gtgtgacaatgagaagGCTcaaaggtcgtccaag-3'). Combination mutants were generated with the following primers: S490A/T494A (5'-ggttctaagaggctgGcgaggagtgtgGcaatgagaagag-3'), T494A/S498A (5'-gctgtcaggagtgtgGcaatgagaagGCTcaaaggtcgtccaag-3'), S490A/S498A (5'-GGTTCTAAGAGGCTGGCGAGGAGTGTGACAATGAGAAAGGCTCAAAGGTCGTCCAAGG-3'), S490A/T494A/S498A (5'-GGCTGGCGAGGAGTGTG-GCAATGAGAAAGGCTCAA-3'). Gain of function mutant (T494E/S498E) was generated by 5'-GTCGAGGAGTGTG-GAAATGAGAAAGGAGCAAAGGTCGTCCAAGGGCTCTG-3'. DNA sequences were confirmed by automated sequencing.

Ca²⁺ Measurements Using Fluo-3—COS-7 cells were incubated with a loading solution consisting of HEPES-buffered saline (HBS; 135 mM NaCl, 5.9 mM KCl, 1.2 mM MgCl₂, 1.5 mM CaCl₂, 11.6 mM HEPES, and 11.5 mM glucose, pH 7.3) supplemented with 2 μ M fluo-3/AM, 0.02% pluronic F-127, and 1 mg/ml bovine serum albumin for 30 min and then incubated in the loading solution without Fluo-3 for 30 min to allow de-esterification of the probe. Loading solution was then replaced with HBS, and cells were placed in a fluorometer (Fluostar) and subjected to the appropriate treatment protocols. Fluorescence intensity (F) was converted into intracellular [Ca²⁺] by using the equation,

$$[\text{Ca}^{2+}] (\text{nM}) = K_d \left(\frac{F - F_{\min}}{F_{\max} - F} \right) \quad (\text{Eq. 1})$$

where F_{\max} was the fluorescence intensity in the presence of 0.1% Triton X-100 and 2 mM CaCl₂, F_{\min} was the fluorescence intensity in the presence of 0.1% Triton X-100 and 1 mM EGTA, and K_d was the dissociation constant for Fluo-3 (390 nM) (15).

Live Cell Imaging—COS-7 cells were transfected with cDNAs encoding fusion proteins of EGFP and monomeric RFP (16) as described above. 24–48 h later, cells were replated onto glass-bottomed dishes (Matek). All imaging was performed using the LSM 510 Meta 3.2 confocal microscope (Zeiss) (Cell Imaging Core, Medical College of Georgia). Magnification power was set at $\times 40$ with oil. Rhodamine phalloidin was obtained from Molecular Probes/Invitrogen.

Immunoblotting—Cell lysates were size-fractionated by SDS-PAGE as described previously (17) and immunoblotted with antibodies to HA (Roche Applied Science); phosphoryl-

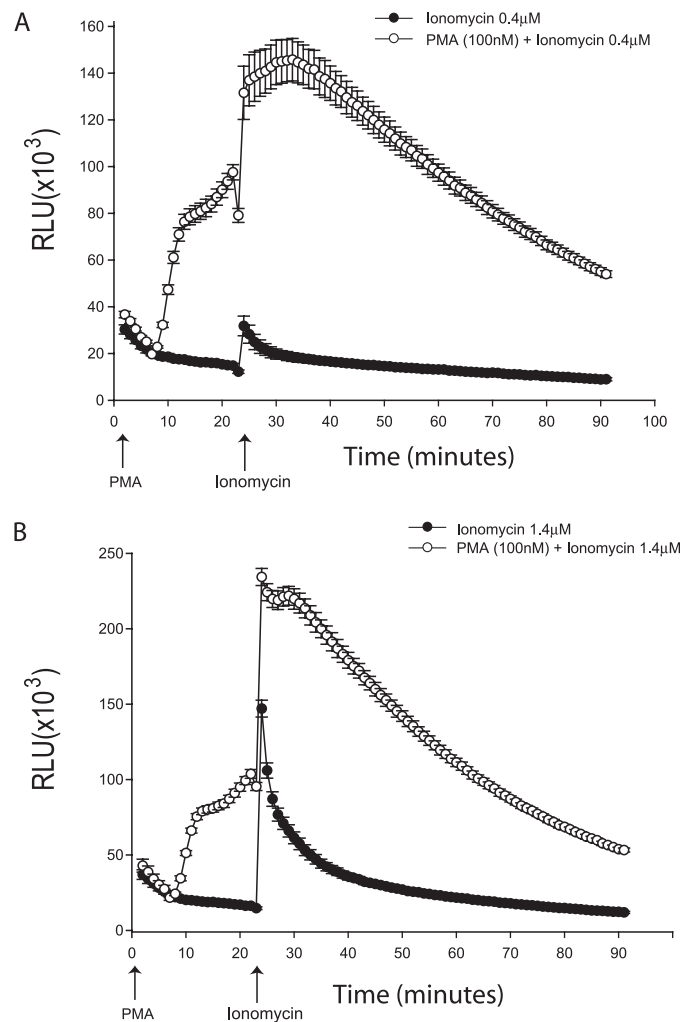


FIGURE 2. PMA pretreatment enhances the sensitivity of Nox5 to ionomycin. COS-7 cells were transfected with Nox5 as described, and cells were treated with or without PMA (100 nM) prior to stimulation with ionomycin. Cells were stimulated with a low concentration of ionomycin (0.4 μ M) (A) or a high concentration (1.4 μ M) (B). The arrows indicate relative times of agonist injection (means \pm S.E., $n = 4$). Results are representative of three independent experiments.

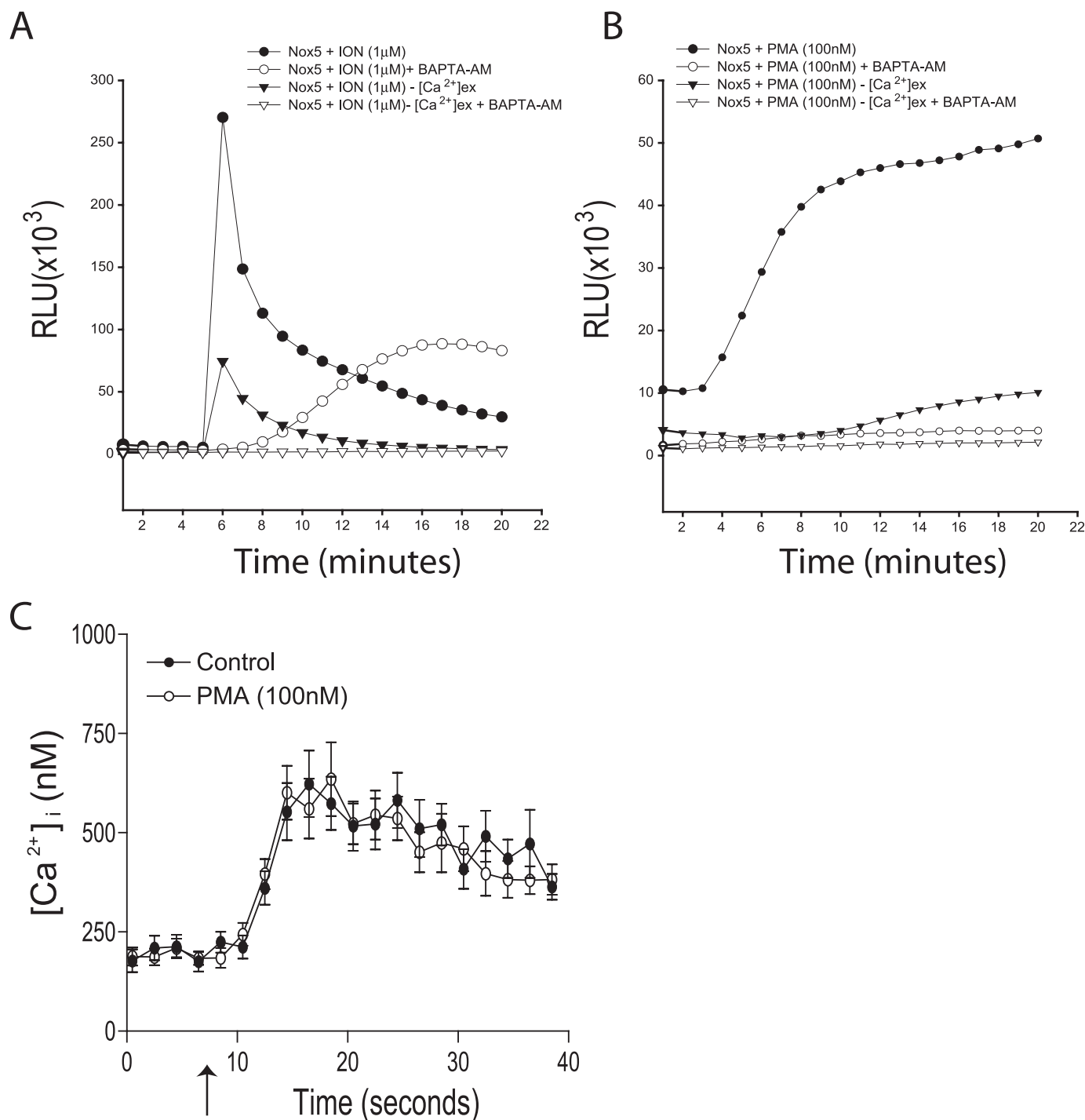


FIGURE 3. PMA-dependent activation of Nox5 is calcium-dependent without a change in intracellular calcium. Nox5-transfected COS-7 cells were stimulated with ionomycin (A) (1 μ M) and PMA (B) (100 nM) in the presence and absence of EGTA (1 mM) to chelate extracellular calcium ($n = 4$) and 1,2-bis(2-aminophenoxy)ethane-*N,N,N',N'*-tetraacetic acid acetoxymethyl ester (BAPTA-AM) (10 μ M) to chelate intracellular calcium ($n = 4$). Results are presented as means to improve clarity. C, COS-7 cells were loaded with the intracellular calcium indicator Fluo3-AM and pretreated with or without PMA (100 nM) and then stimulated with ionomycin (1 μ M; means \pm S.E., $n = 12$).

ated PKC substrate (Cell Signaling), which recognizes the motif (R/K)XS*X(R/K) where X represents any amino acid and S* is phosphoserine; hsp90; PTP1B; Vimentin; and poly-(ADP-ribose) polymerase (BD Biosciences). Phosphorylation state-specific antibodies to Thr⁴⁹⁴ and Ser⁴⁹⁸ were generated by Pacific Immunology using the following epitopes (threonine 494, C-SKRLRSVT*MRSKQRS; serine 498,

C-LSRSVTMRKS*QRSSKGS). Antibodies were affinity-purified by negative selection (dephosphopeptide column) and positive selection (phosphopeptide column). The specificity of these antibodies was determined against the full-length Nox5 protein as shown in Fig. 10, B and C.

Subcellular Fractionation—The relative subcellular location of Nox5 was determined using the subcellular proteome extrac-

Activation of Nox5 via Phosphorylation

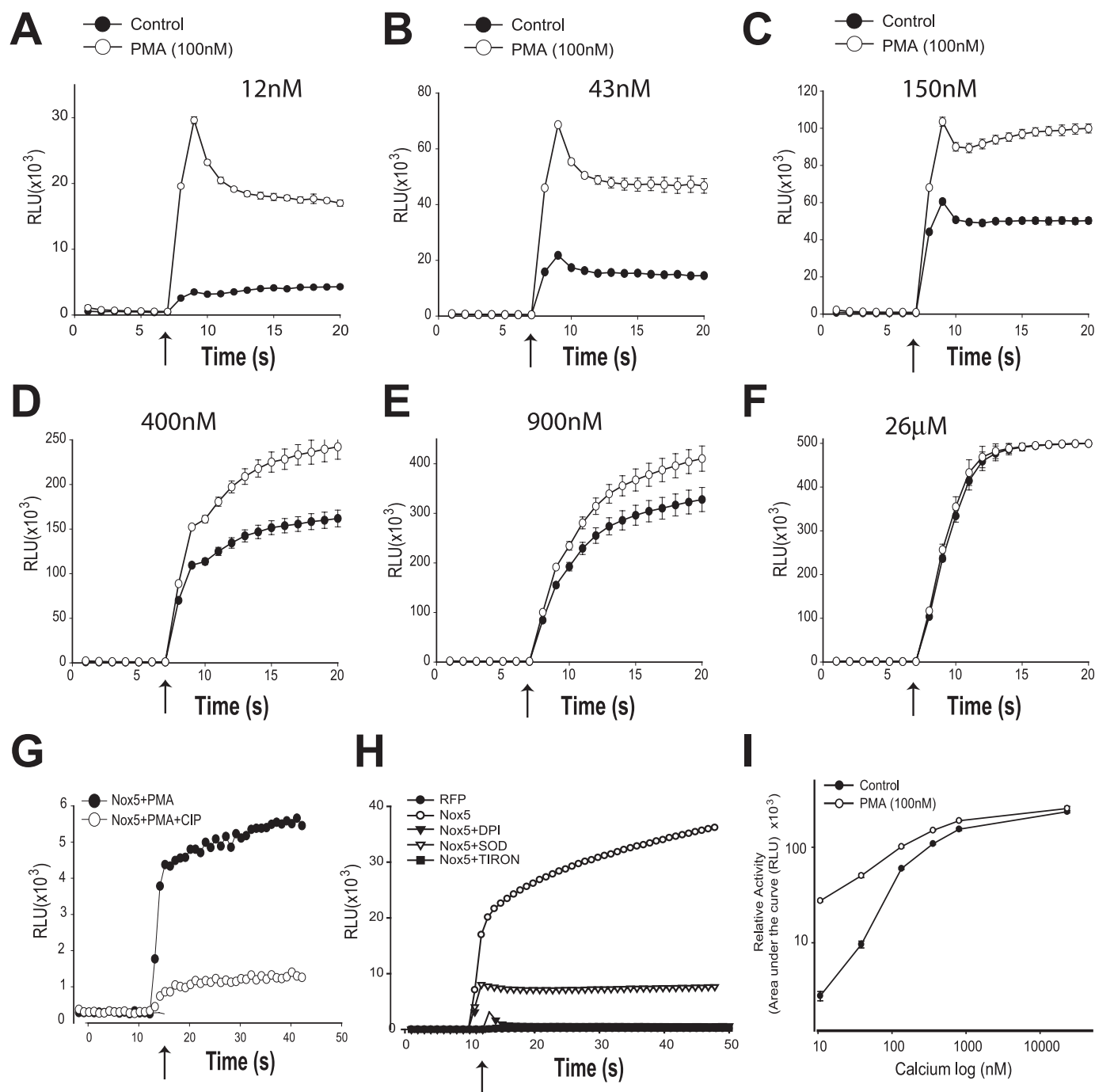


FIGURE 4. PMA directly modifies Nox5 activity. COS-7 cells were stimulated with PMA (100 nM) or vehicle for 60 min, and the activity of Nox5 in cell-free extracts was determined in the presence of different concentrations of free calcium (A–F) (means \pm S.E., $n = 2$). The arrows indicate injection of NADPH (200 μ M). G, PMA-treated cell extracts were exposed to alkaline phosphatase (CIP) (50 units) or vehicle (glycerol) for 60 min at 25 $^{\circ}$ C and then incubated with 43 nM free calcium ($n = 3$) prior to activation. H, COS-7 cells were transfected with RFP (control, $n = 4$) or Nox5 cDNA ($n = 4$) and then preincubated with either vehicle, DPI (10 μ M, $n = 3$), SOD (100 units/ml, $n = 3$), or TIRON (5 mM, $n = 3$). Results are representative of three independent experiments. I, the areas under the curve from the experiments (A–F) are plotted against the calcium concentration.

tion kit (Calbiochem). Confluent 100-mm dishes of COS-7 cells transfected with Nox5 were exposed to PMA (100 nM), α -PMA, or ionomycin and separated into cytosol, membrane, nucleus, and cytoskeleton fractions according to the manufacturer's instructions. In brief, adherent cells were washed with ice-cold wash buffer and then sequentially extracted using a combination of four extraction buffers. Each fraction recovered was then immunoblotted with antibodies against cytosolic, membrane, nuclear,

and cytoskeleton proteins to verify the procedure. To determine the detergent solubility of Nox5, cells were lysed in a buffer (pH 7.5, 50 mM Tris-HCl, 0.1 mM EDTA, 0.1 mM EGTA, 0.1% SDS, 0.1% deoxycholic acid, and 1% Triton), sonicated (6×1 -s bursts on level 5), and separated by centrifugation ($20,000 \times g$ for 10 min) into soluble and insoluble fractions.

Cell-free Activity Assays—COS-7 cells expressing Nox5 were lysed in a MOPS (30 mM, pH 7.2)-based buffer containing KCl

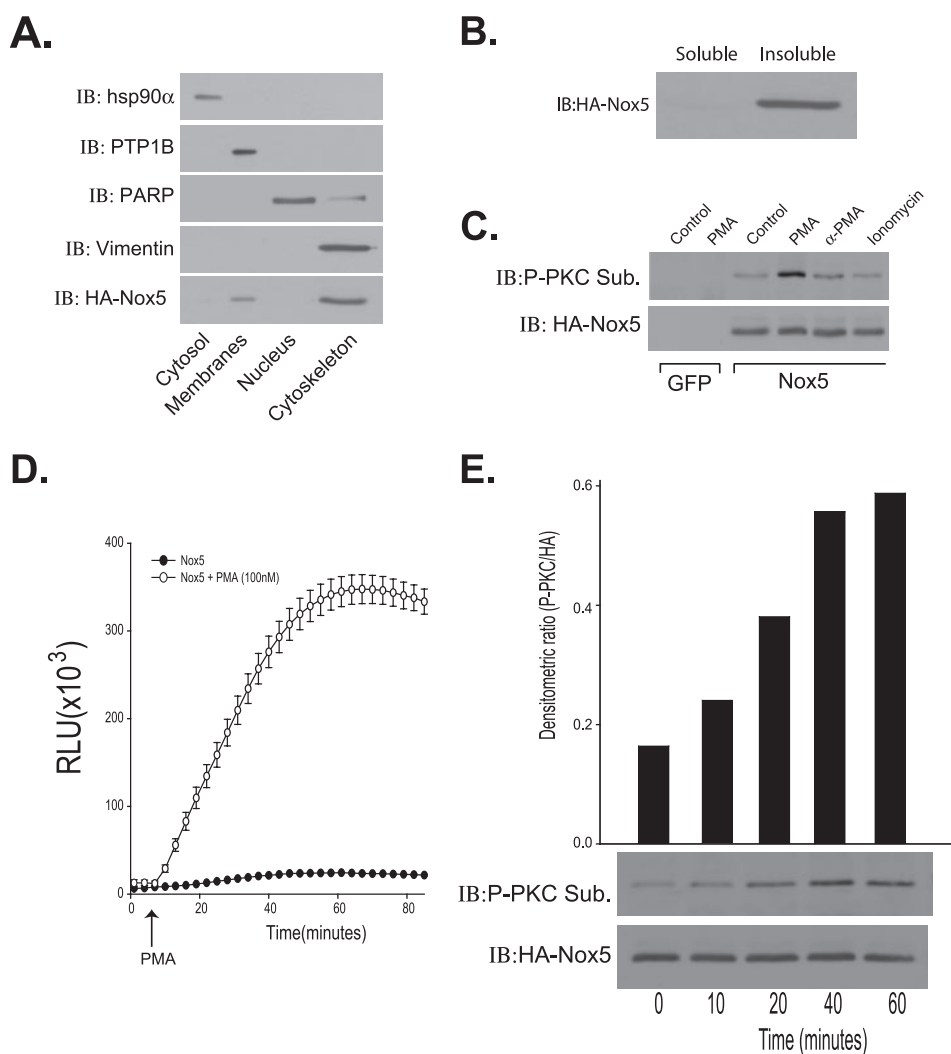


FIGURE 5. Nox5 is present within the cytoskeletal fraction and is phosphorylated by PMA in a time-dependent manner. *A*, subcellular fractionation of COS-7 cells expressing Nox5. Fractions containing cytosolic, membrane, nuclear, and cytoskeletal proteins were confirmed by the presence of hsp90 α , PTP-1B, poly(ADP-ribose) polymerase, and vimentin, respectively. *B*, COS-7 cells expressing Nox5 were separated into Triton (1%) soluble and -insoluble fractions. *C*, detection of phosphorylated Nox5 in the cytoskeletal fraction in response to β -PMA (100 nM), α -PMA, or ionomycin. *D*, time-dependent increase in Nox5 activity ($n = 4$) and phosphorylation in response to PMA (100 nM) (means \pm S.E., $n = 2$). *E*, relative densitometry of phosphorylated Nox5 compared with total protein (0–60 min). *IB*, immunoblot.

(100 mM), Triton (0.3%), and protease inhibitors (Sigma). Adherent cells were rocked gently, and the lysis buffer was aspirated and then washed three times with phosphate-buffered saline (4 $^{\circ}$ C). Remaining cytoskeletal fractions were resuspended in the above MOPS buffer containing 0.3 mM EGTA to remove any residual calcium. These fractions were sonicated at low power and spun down at 14,000 rpm (4 $^{\circ}$ C). The supernatant was then aspirated, and the pellet was resuspended in MOPS buffer with mild sonication. The cell-free extract was aliquoted into buffers containing L012 (400 μ M), 1 mM MgCl₂, 100 μ M FAD (Sigma), and buffered free calcium ranging from 0 to 26 μ M (Invitrogen/Molecular Probes calcium calibration buffer kit). In select experiments, 50 units of calf intestinal phosphatase (CIP) (New England Biolabs) or glycerol (vehicle control, 5 μ l) were added and incubated at 25 $^{\circ}$ C for 1 h prior to the addition of calcium. After a brief period of equilibration, reduced NADPH (Sigma) was injected to a final concentration

of 200 μ M, and the production of reactive oxygen species was monitored over time. LY379196 was a generous gift from Lilly.

Statistical Analysis—Luminescence data are expressed as mean \pm S.E. All analyses were performed using GraphPad InStat software (GraphPad Software, Inc.) and were made using a two-tailed Student's *t* test or analysis of variance with a *post hoc* test where appropriate. Differences were considered as significant at $p < 0.05$ (*).

RESULTS

Activation of Nox5 by Distinct Mechanisms—As shown previously, the activity of Nox5 can be acutely regulated by elevating intracellular calcium. In Fig. 1*A*, the addition of ionomycin triggers a rapid increase in the production of ROS compared with cells treated with vehicle. In the presence of the flavoprotein inhibitor, diphenyleneiodonium (DPI), and the superoxide scavengers, SOD and TIRON, this signal is eliminated, indicating that it derives from a Nox (Fig. 1*B*). However, as shown in Fig. 1*C*, the addition of β -PMA induces a slow and sustained production of ROS that is evident over 1 h. The inactive structural analogue of β -PMA, α -PMA, did not stimulate ROS production. Furthermore, DPI, SOD, and TIRON all abolished PMA-dependent ROS production, confirming Nox as the source of ROS (Fig. 1*D*). A direct comparison of cells

expressing Nox5 *versus* a control cDNA, GFP, revealed that all of the ROS produced in response to both PMA and ionomycin derives from Nox5 (Fig. 1*E*).

Preexposure of PMA Potentiates Calcium-dependent Nox5 Activity—To investigate the interrelationship, if any, between the activation of Nox5 with ionomycin *versus* PMA, COS-7 cells expressing Nox5 were challenged with PMA prior to the addition of different concentrations of ionomycin. As shown in Fig. 2*A*, the addition of a relatively low concentration of ionomycin (400 nM) stimulates a small net increase in Nox5 activity of $\sim 20 \times 10^3 \pm 4 \times 10^3$ RLU. The preexposure of PMA increases base-line ROS-dependent luminescence from 16×10^3 to $80\text{--}90 \times 10^3$, but interestingly, PMA potentiated the low dose ionomycin (400 nM) response to a net of $67 \times 10^3 \pm 7 \times 10^3$ RLU, or 3.5-fold higher than in the absence of PMA ($p < 0.05$). With higher concentrations of ionomycin (1.4 μ M), there is a much more robust increase in net Nox5 activity of $\sim 132 \times$

Activation of Nox5 via Phosphorylation

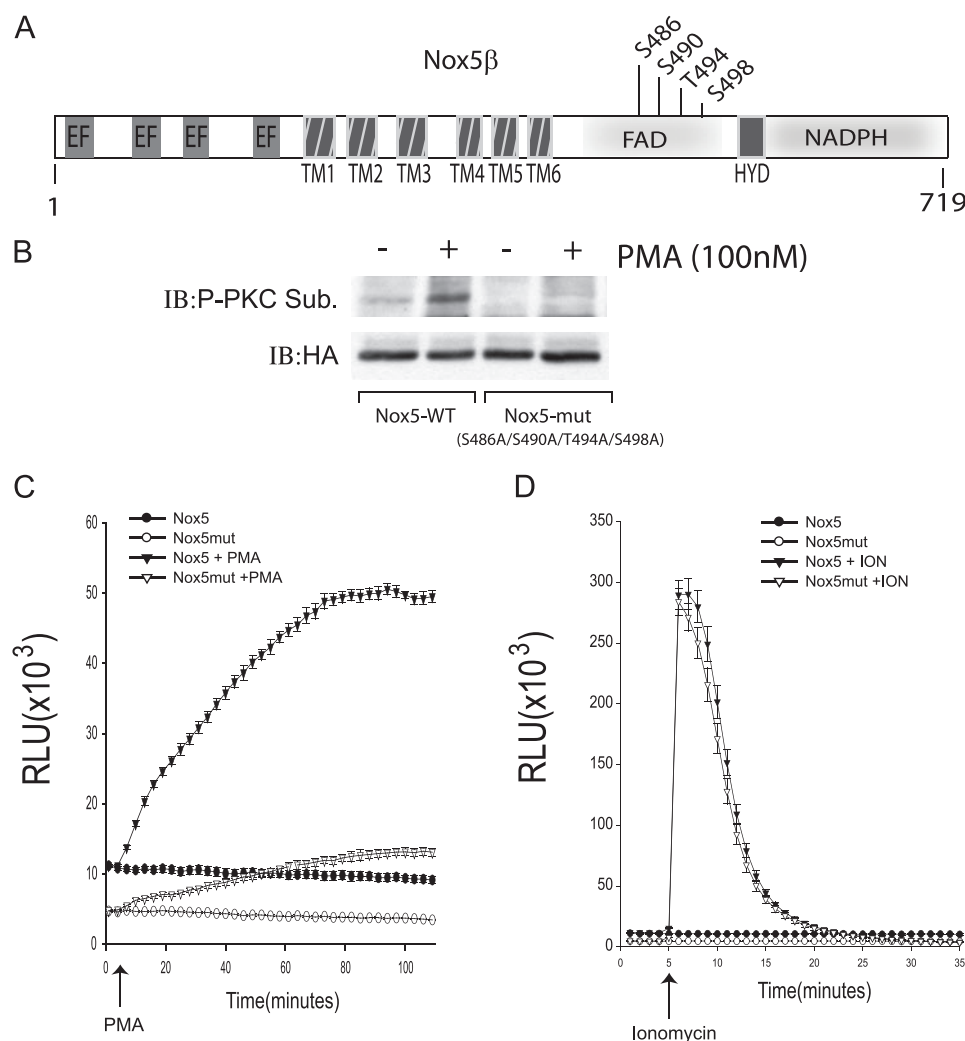


FIGURE 6. Mutation of putative Nox5 phosphorylation sites inhibits phosphorylation- and PMA-dependent activation. *A*, schematic illustrating position of putative Nox5 phosphorylation sites (*TM*, transmembrane domains; *HYD*, hydrophobic helix; *EF*, EF hands). *B*, COS-7 cells expressing WT and mutant (S486A/S490A/T494A/S498A) Nox5 were stimulated with PMA (100 nM), and the phosphorylation level was determined in the cytoskeletal fraction. Results are representative of at least three separate experiments. COS-7 cells expressing WT and mutant Nox5 were stimulated with PMA (100 nM) (*C*) or ionomycin (1 μ M) (*D*) (means \pm S.E., $n = 4$).

$10^3 \pm 5 \times 10^3$ RLU (Fig. 2*B*). Preincubation with PMA increased base-line Nox5 activity to equivalent levels as shown in Fig. 2*A*, but the net ionomycin stimulation in excess of the PMA response was $139 \times 10^3 \pm 4 \times 10^3$ and not significantly different from that in the absence of PMA. Even more striking was the ability of PMA to potentiate the duration of Nox5 activation as estimated from the area under the curve above base line following ionomycin stimulation. In response to the low dose of ionomycin, the area under the curve in the presence of PMA was 16-fold greater compared with control cells (using the elevated PMA level as base line). For the higher dose of ionomycin, this difference was less apparent and only 3-fold greater in the PMA-treated group.

Activation of Nox5 by PMA Is Direct and Dependent on Intra- and Extracellular Calcium—COS-7 cells expressing Nox5 were pretreated with EGTA (2 mM) or 1,2-bis(2-aminophenoxy)ethane-*N,N,N',N'*-tetraacetic acid acetoxymethyl ester (10 μ M) and stimulated with ionomycin (1 μ M) or PMA (100 nM). As shown in Fig. 3*A*, intracellular and extracellular calcium

are both required for full activation of Nox5 in response to ionomycin. Chelation of intracellular calcium reduced the maximum activity of Nox5 and delayed the kinetics of activation. Removal of extracellular calcium did not affect the speed of activation but reduced maximum activity. The combination of the two chelators completely abrogated activity. The response to PMA was completely calcium-dependent, since chelation of either intracellular or extracellular calcium virtually abolished Nox5 activity (Fig. 3*B*). To exclude the possibility that PMA is elevating intracellular calcium and secondarily activating Nox5, we next measured the level of intracellular calcium using the fluorescent intracellular calcium probe, Fluo-3. As shown in Fig. 3*C*, PMA does not modify the resting level of intracellular calcium or the increase in response to ionomycin as shown by the measurement of calcium over time. In addition, the net increase in intracellular calcium in response to lower concentrations of ionomycin (100 nM) was not affected by PMA (data not shown).

To identify whether PMA was inducing a direct change in Nox5 activity, we next performed activity assays in cell-free conditions. As shown in Fig. 4, *A–F*, Nox5 isolated from PMA-treated cells exhibited an increase in calcium sensitivity compared with vehicle-treated

cells. With sufficient calcium, the activity of control and PMA-treated Nox5 was equivalent (Fig. 4*F*). To evaluate whether phosphorylation was responsible for the change in calcium sensitivity, cell extracts were pretreated with CIP to dephosphorylate Nox5. As shown in Fig. 4*G*, CIP reduced the calcium sensitivity of Nox5, demonstrating that phosphorylation is required for the calcium sensitization. The cell-free assay was specific for Nox5 activity, since there was no ROS production in COS-7 cells expressing only a control plasmid and also since ROS production in cells expressing Nox5 was attenuated by DPI, SOD, and TIRON (Fig. 4*H*). The relative increase in calcium-dependent activity in cells exposed to PMA *versus* vehicle is shown in Fig. 4*I* ($p < 0.05$).

Nox5 Is Present in the Cytoskeletal Fraction and Is Phosphorylated by PMA—COS-7 cells expressing Nox5 were separated into cytosolic, membrane, nuclear, and cytoskeletal fractions. As shown in Fig. 5*A*, Nox5 is present primarily in the cytoskeletal fraction, with a small amount detected in the membrane fraction. The validity of our fractionation methodology was

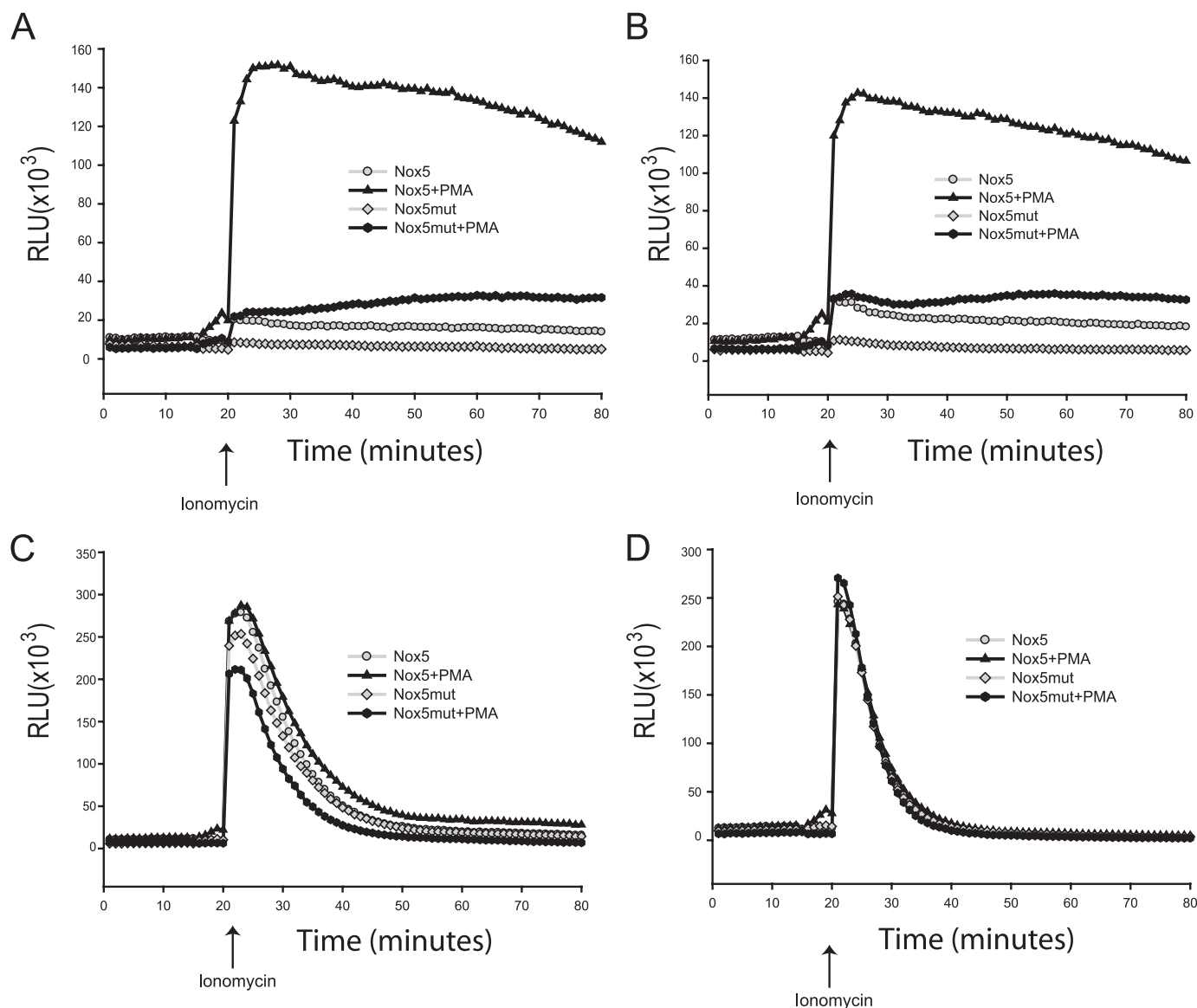


FIGURE 7. **Nox5 calcium sensitization is dependent on PMA phosphorylation sites.** COS-7 cells expressing WT Nox5 or a Nox5 phospho-null mutant (S486A/S490A/T494A/S498A) were pretreated with PMA (100 nM) or vehicle prior to activation with different concentrations of ionomycin. *A*, 0.2 μM ; *B*, 0.4 μM ; *C*, 0.6 μM ; *D*, 1.2 μM (means \pm S.E., $n = 5$). The arrows indicate ionomycin injection.

confirmed by the presence of hsp90 α in the cytosol, PTP-1B in membranes, poly(ADP-ribose) polymerase in the nucleus, and vimentin in the cytoskeletal fraction (Fig. 5A). To confirm that Nox5 was present in the detergent-insoluble fraction, cells were lysed in a 1% Triton buffer and separated via centrifugation into equal volume soluble and insoluble fractions. As shown in Fig. 5B, virtually all of the Nox5 was present in the detergent-insoluble fraction. Thus, the detergent-resistant nature of Nox5 and its presence in the cytoskeletal fraction precluded us from using immunoprecipitation to isolate Nox5 from other proteins and determine its phosphorylation state. Instead, we exploited this subcellular fractionation technique to partially purify Nox5 in the cytoskeletal fraction and thus determine its phosphorylation state using an anti-PKC substrate antibody. Fig. 5C demonstrates that upon stimulation with PMA, but not α -PMA or ionomycin, Nox5 is robustly phosphorylated. Notably, in COS-7 cells transfected with a control plasmid, GFP, there was

no detectable signal in this fraction at the same molecular weight as Nox5. To correlate phosphorylation with ROS generation, we directly compared the activity of Nox5 (Fig. 5D) with its phosphorylation state (Fig. 5E). Exposure of cells to PMA induced the time-dependent phosphorylation of Nox5, which was maximal between 40 and 60 min and matched precisely the time-dependent increase in Nox5 activity.

The Phosphorylation of Nox5 on Specific Residues Regulates Its Activity—Our next goal was to identify putative Nox5 phosphorylation sites. Using motif scanning for PKC substrates, based on the consensus motif of RXS/TXR and the program DIPHOS, a cluster of potential PKC phosphorylation sites was identified at Ser⁴⁸⁶, Ser⁴⁹⁰, Thr⁴⁹⁴, and Ser⁴⁹⁸ (Fig. 6A). Site-directed mutagenesis of these phosphorylation sites completely abolished both basal phosphorylation and the ability of PMA to induce phosphorylation (Fig. 6B). To address the functional ramifications of these phosphorylation sites, COS-7 cells were

Activation of Nox5 via Phosphorylation

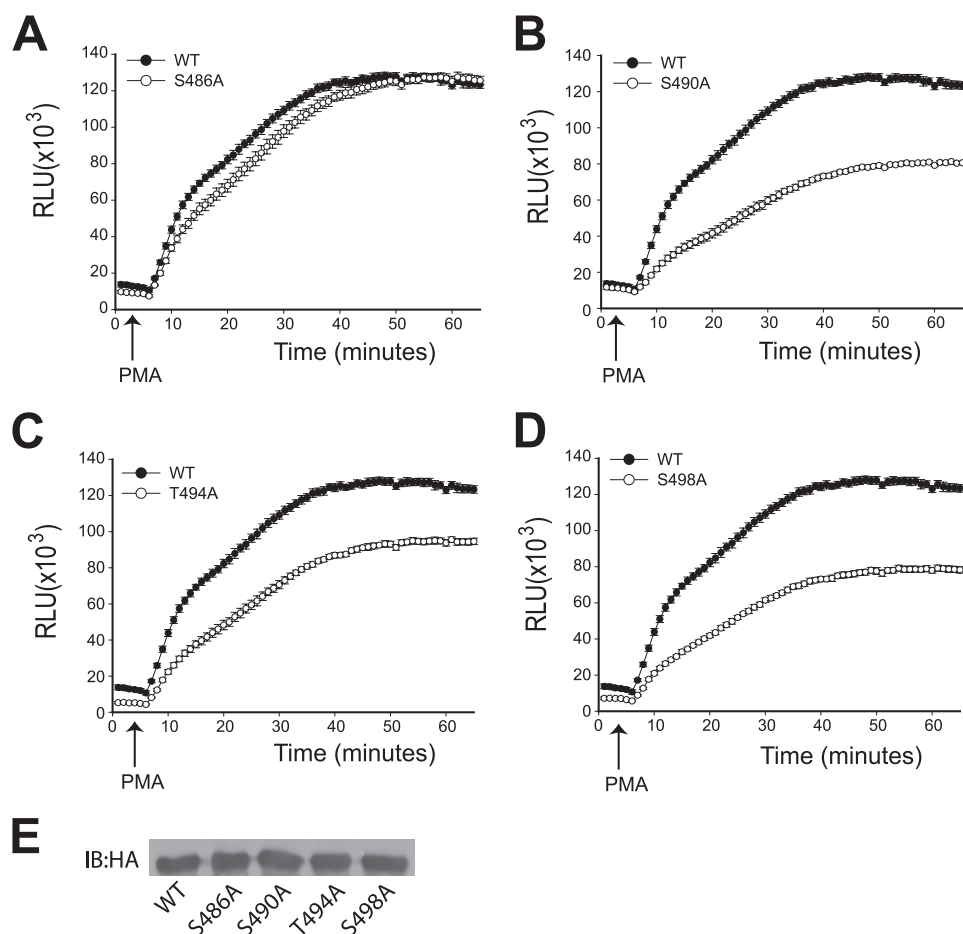


FIGURE 8. Functional relevance of individual Nox5 phosphorylation sites. COS-7 cells expressing either S486A (A), S490A (B), T494A (C), and S498A Nox5 (D) were stimulated with PMA (100 nM), and ROS production was monitored over time as shown (means \pm S.E., $n = 4$). The relative expression level of Nox5 and mutant constructs was determined by immunoblot (IB) (E). Results are representative of three independent experiments.

transfected with WT Nox5 and mutant Nox5 in which Ser⁴⁸⁶, Ser⁴⁹⁰, Thr⁴⁹⁴, and Ser⁴⁹⁸ were mutated to the nonphosphorylatable analogue, alanine. As shown in Fig. 6C, the ability of PMA to stimulate Nox5 activity was greatly attenuated in the phospho-null mutant compared with WT. To address potential negative consequences on overall Nox5 activity, we next examined the ability of high doses of ionomycin to stimulate the calcium-dependent activation. There was no significant difference in the ability of ionomycin to stimulate ROS production from WT and mutant Nox5 (Fig. 6D). This finding demonstrates that the deletion of the PMA-dependent phosphorylation sites selectively reduces ROS generation in response to PMA but does not reduce Nox5 activity *per se*.

Mutation of PMA-dependent Phosphorylation Sites Inhibits Calcium Sensitization—Nox5-transfected COS-7 cells were pretreated with PMA or vehicle and then stimulated with different concentrations of ionomycin. Low concentrations of ionomycin (0.2 μ M) evoked a very small increase in ROS production that was greatly potentiated by pretreatment with PMA (Fig. 7A). This potentiation was greatly reduced in cells expressing the Nox5 phospho-null mutant, where the response to ionomycin was equivalent to that of the WT Nox5 in the absence of PMA. PMA also significantly prolonged the dura-

tion of increased WT Nox5 activity as evident in Fig. 7, A and B. As the concentration of ionomycin increased (Fig. 7, B–D), the effect of PMA diminished. With sufficient ionomycin concentration, the difference between all groups was normalized, demonstrating that the capacity of Nox5 to produce ROS was equivalent, given sufficient calcium.

Identification and Functional Relevance of Specific Nox5 Phosphorylation Sites—To identify the specific sites involved, we individually mutated each of the putative phosphorylation sites and compared the activity to WT. As shown in Fig. 8A, the activity of the S486A mutant was equivalent to that of WT, but mutation of Ser⁴⁹⁰, Thr⁴⁹⁴, and Ser⁴⁹⁸ all produced modest inhibition ranging from 25 to 35% (Fig. 8, B–D). We next addressed whether more than one phosphorylation site was required for full activity. In Fig. 9, A and B, COS-7 cells were transfected with WT and S490A/T494A, T494A/S498A, and S490A/S498A double mutants and simulated with PMA. All double mutants produced substantially greater inhibition than the single mutants, with the T494A/S498A

combination the most effective. The triple mutant (S490A/T494A/S498A) also produced substantial inhibition of PMA-stimulated activity (Fig. 9E). Again, to exclude the possibility that these mutations have spurious effects on the activity of Nox5, we examined the response to high concentrations of ionomycin. As shown in Fig. 9, B, D, and F, the response to ionomycin was not significantly reduced compared with WT.

To identify the specific phosphorylation sites on Nox5 recognized by the phospho-PKC substrate antibody, we performed immunoblots with cell extracts containing WT, S486A, S490A, T494A, or S498A Nox5. As shown in Fig. 10A, the phospho-PKC substrate antibody recognizes exclusively the Ser⁴⁹⁸ site, as demonstrated by the complete loss of signal with only the S498A mutant. To further evaluate the role of these sites, we developed phosphorylation state-specific antibodies to Thr⁴⁹⁴ and Ser⁴⁹⁸. In Fig. 10B, we show that PMA induces the robust phosphorylation of Ser⁴⁹⁸. The specificity of this antibody is demonstrated by the reduced signal seen following treatment with CIP and elimination in the presence of the alanine mutant. Similarly, the phosphorylation of Thr⁴⁹⁴ is increased in response to PMA and abolished by CIP treatment or mutation (Fig. 10C). To further establish the functional significance of these residues, we

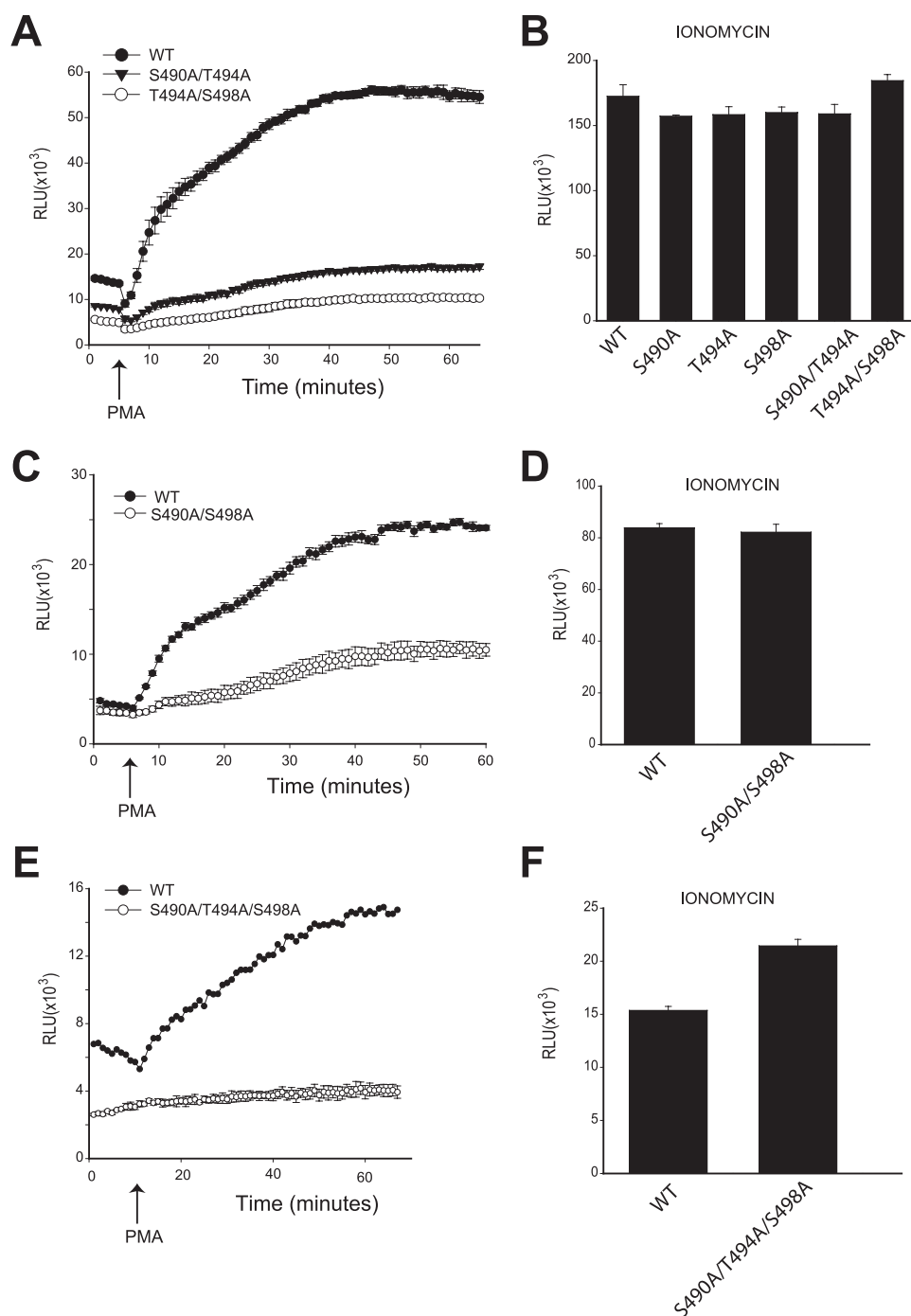


FIGURE 9. Phosphorylation of more than one phosphorylation site is required for full Nox5 activity in response to PMA. A, COS-7 cells expressing WT, S490A/T494A, and T494A/S498A Nox5 were stimulated with PMA (100 nM, means \pm S.E., $n = 4$). B, relative activity of WT, S486A, S490A, T494A, S498A, S490/T494A, and T494/S498A Nox5 in the presence of ionomycin (1 μ M, means \pm S.E., $n = 5$). C, COS-7 cells expressing WT and S490A/S498A Nox5 were stimulated with PMA (100 nM, means \pm S.E., $n = 4$). D, relative activity of WT and S490A/S498A Nox5 in the presence of ionomycin (1 μ M, means \pm S.E., $n = 5$). E, COS-7 cells expressing WT and S490A/T494A/S498A Nox5 were stimulated with PMA (100 nM, means \pm S.E., $n = 4$). F, relative activity of WT and S490A/S498A/S498A Nox5 in the presence of ionomycin (1 μ M, means \pm S.E., $n = 4$).

mutated Thr⁴⁹⁴ and Ser⁴⁹⁸ to the phospho-mimetic residue, glutamic acid. COS-7 cells expressing the T494E/S498E mutant produced significantly more ROS in response to low concentrations of ionomycin, despite the presence of equivalent amounts of protein (Fig. 10, D and E).

bulin and F-actin (Fig. 12, F and G).

DISCUSSION

The variety and intricacy of the mechanisms controlling the activity of NADPH oxidases is remarkable. Nox1 to -4 require

Influence of PKC Inhibitors on Nox5 Activity—To determine whether PMA-dependent activation of Nox5 involves PKC, COS-7 cells expressing Nox5 were incubated with the PKC inhibitors rottlerin and LY379196. Both rottlerin and LY379196 significantly attenuated PMA-dependent increases in Nox5 activity (Fig. 11A); however, rottlerin also inhibited the response to ionomycin (Fig. 11B), indicating that its actions may not be entirely specific for PKC. Furthermore, LY379196 significantly reduced the phosphorylation of Ser⁴⁹⁸ and to a lesser extent Thr⁴⁹⁴. These results indicate that PKC- β or a similar isoform participates in the phosphorylation and activation of Nox5.

Identification of the Subcellular Location of Nox5—To characterize the location of Nox5 within COS-7 cells, we generated N-terminal GFP and RFP Nox5 fusion proteins. Importantly, these proteins were still active and produced ROS in response to both ionomycin and PMA (data not shown). In transfected COS-7 cells, Nox5-GFP exhibited a pronounced perinuclear staining pattern with an extensive network of branching tubules that project into the cytosol (Fig. 12A). Although perinuclear in appearance, Nox5 did not appreciably colocalize with subcellular markers for the Golgi or the mitochondria (Fig. 12, C and E). Nox5 was also absent from the nucleus and the plasma membrane (Fig. 12, A and B). However, considerable overlap was detected with the marker for the endoplasmic reticulum (Fig. 12D). Although we had originally detected Nox5 in the cytoskeletal fraction using subcellular fractionation, confocal microscopy revealed that it does not overlap with markers for the cytoskeleton, including both α -tu-

Activation of Nox5 via Phosphorylation

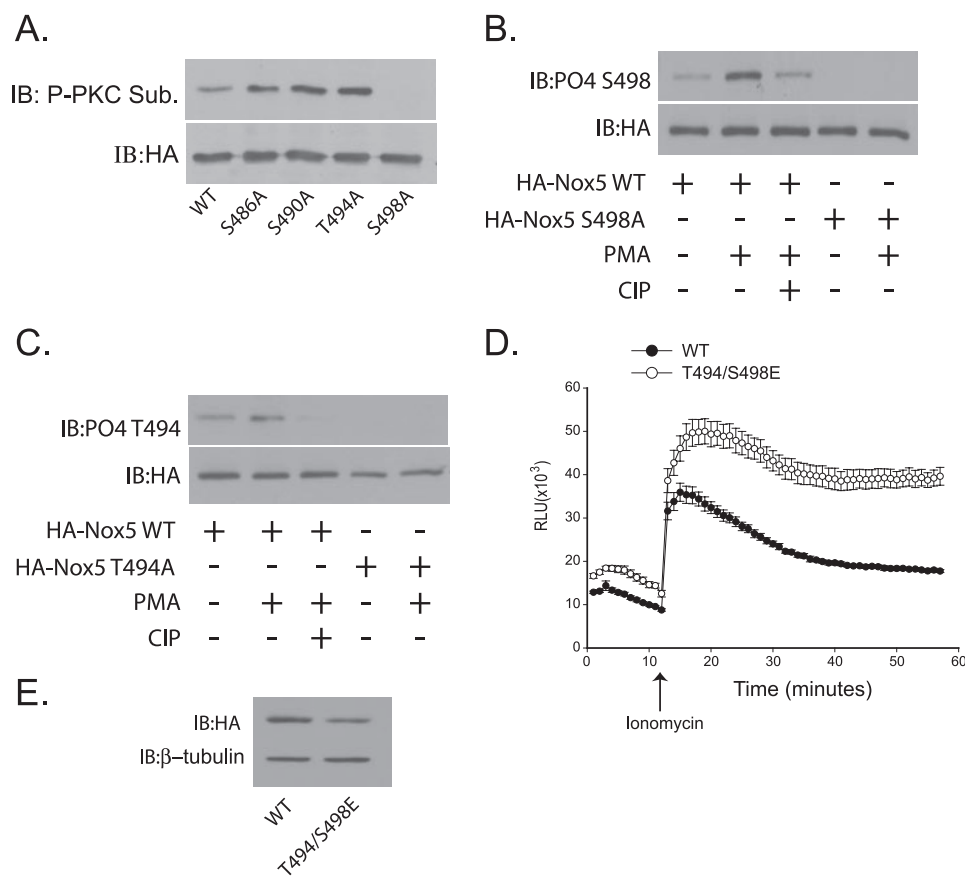


FIGURE 10. Identification of Nox5 phosphorylation sites. A, COS-7 cells expressing WT, S486A, S490A, T494A, or S498A Nox5 were stimulated with PMA (100 nM), and the cytoskeletal fraction was immunoblotted (IB) for phosphorylated PKC substrate antibody (top) relative to total Nox5 (HA) (bottom). B, COS-7 cells expressing WT or S498A Nox5 were stimulated with PMA (100 nM) and immunoblotted for phosphorylated S498 (top) relative to total Nox5 (HA) (bottom). In additional experiments, cell extracts containing Nox5 were exposed to CIP (50 units) or vehicle (glycerol) for 60 min at 25 °C and immunoblotted as described. In C, COS-7 cells expressing WT or T494A Nox5 were stimulated with PMA (100 nM) and immunoblotted for phosphorylated T494 (top) relative to total Nox5 (HA) (bottom). D, relative activity of WT and T494E/S498E mutant Nox5 in response to a low concentration of ionomycin (400 nM, means \pm S.E., $n = 4$). E, relative expression of WT and T494A/S498E (top) versus loading control β -tubulin (bottom).

the presence of accessory proteins, p22^{phox}, p47^{phox}, p40^{phox}, p67^{phox}, Rac, NOXO1, and NOXA1, in various proportions to fully activate superoxide production (3). Nox5 is different altogether. Currently, it appears that Nox5 can operate independently of any of the accessory proteins described for the other Noxs (11). Instead, the activity of Nox5 is driven acutely by the elevation of intracellular calcium. In addition, the production of superoxide from Nox5 is comparatively transient (minutes) compared with the long lasting activation (minutes to hours) exhibited by the other Noxs. However, the level of intracellular calcium required for activation of Nox5 is relatively high at 1–10 μ M for half and maximum activation, respectively, which raises the question of whether cells regularly experience sufficient calcium for Nox5 activation (11). In the current paper, we have identified a novel mechanism that regulates the activity of Nox5 by increasing its sensitivity to lower levels of intracellular calcium and by prolonging the duration of superoxide production.

PMA treatment of cells expressing Nox5 resulted in a slow and steady production of ROS above base line. This differs significantly from the transient nature of the response to ionomycin. The combination of PMA and ionomycin, how-

ever, results in a clear potentiation of both the amplitude and duration of ROS production, particularly at low concentrations of ionomycin. The ability of PMA to potentiate the ionomycin response diminished with increasing concentration of ionomycin and was completely dependent on calcium, since chelation of both intra- and extracellular calcium abolished this effect. This ability of PMA to stimulate Nox5 activity was a direct effect on the enzyme, since prior exposure of cells to PMA sensitizes Nox5 to calcium in cell-free activity assays. This calcium sensitization was reversed by treatment with alkaline phosphatase, providing evidence that direct phosphorylation of Nox5 mediates this effect. Furthermore, PMA did not modify the concentration of intracellular calcium, either under basal conditions or in the presence of ionomycin. Collectively, these results support the hypothesis that PMA enhances the calcium sensitivity of Nox5.

In response to PMA, we also detected the time-dependent phosphorylation of Nox5. Mutation of putative serine and threonine residues (Ser⁴⁸⁶, Ser⁴⁹⁰, Thr⁴⁹⁴, and Ser⁴⁹⁸) to the nonphosphorylatable analogue, alanine, prevented both

the phosphorylation, the PMA-dependent increase in ROS production and the ability of PMA to potentiate ROS production at low concentrations of ionomycin. To exclude the possibility that these mutations simply cripple Nox activity in response to all stimuli, we show that in the presence of higher concentrations of ionomycin, the total activity of the Nox5 phospho-null mutant was equivalent to that of WT. Therefore, in the presence of sufficient calcium ions, Nox5 is no longer dependent on the phosphorylation of these sites for full activity. Individual mutation of these phosphorylation sites produced only slight inhibition, suggesting that they may function cooperatively. In support of this concept, double mutations (S490A/T494A, S490A/S498A, or T494A/S498A) and triple mutants (S490A/T494A/S498A) resulted in substantially less PMA-dependent activity. Mutation of Thr⁴⁹⁴/Ser⁴⁹⁸ to the phosphomimetic glutamic acid produced a gain of function mutant that exhibited greater activity in response to lower concentrations of ionomycin and provides strong evidence that the phosphorylation of this region regulates Nox5 activity. To identify the specific sites of phosphorylation, we generated phosphorylation state-specific antibodies to Thr⁴⁹⁴ and Ser⁴⁹⁸ and characterized the specificity of the phospho-PKC substrate antibody using site-di-

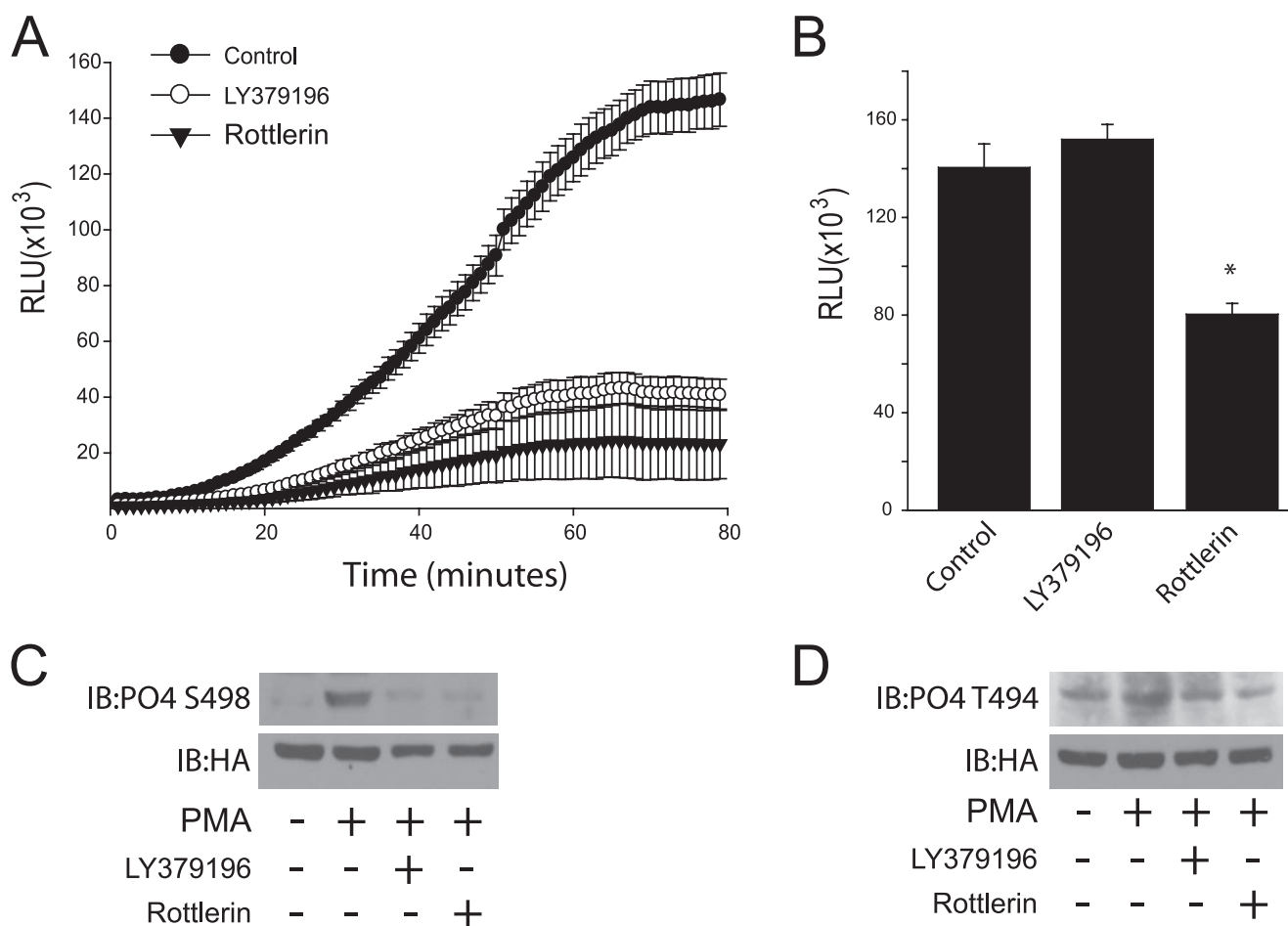


FIGURE 11. Inhibition of Nox5 activity and phosphorylation by PKC inhibitors. COS-7 cells expressing Nox5 were pretreated with vehicle (Me₂SO), LY379196 (200 nM), or rottlerin (1 μ M) for 30 min prior to stimulation with PMA (A, 100 nM) or ionomycin (B, 1 μ M), and production of ROS was monitored over the times indicated (means \pm S.E., $n = 5$). C and D, the ability of LY379196 (200 nM) or rottlerin (1 μ M) to modulate PMA-dependent phosphorylation of Thr⁴⁹⁴ or Ser⁴⁹⁸ was determined by immunoblotting (IB) (top) relative to the level of total Nox5 protein (bottom).

rected mutants. We show that the phospho-PKC antibody recognizes only phosphorylated Ser⁴⁹⁸. Moreover, using the phosphorylated antibodies to Thr⁴⁹⁴ and Ser⁴⁹⁸, we show that PMA induces the site-specific phosphorylation of Thr⁴⁹⁴ and Ser⁴⁹⁸. The kinase responsible for the phosphorylation of Nox5 is not yet identified. However, both phosphorylation and PMA-dependent increases in activity were susceptible to the specific PKC- β inhibitor (LY379196), suggesting that PKC- β or a similar PKC isoform mediates this effect.

The molecular mechanisms by which phosphorylation of Nox5 facilitates the calcium-dependent synthesis of ROS are unknown. Previously, it has been shown that the N-terminal EF hands of Nox5 interact with its C terminus to facilitate ROS production. The binding of calcium to the EF hands of Nox5 induces a conformational change that exposes a hydrophobic region. This region then combines with a yet to be identified C-terminal domain, leading to increased electron transport and ROS production (11). In the presence of PMA, both the amplitude and duration of the calcium-dependent Nox5 activity are enhanced. It is therefore conceivable that phosphorylation facilitates or stabilizes the interaction between these two protein domains and that more than one phosphorylation site is required to mediate this process. As depicted in Fig. 6A, the Thr⁴⁹⁴ and Ser⁴⁹⁸ phosphorylation sites lie outside of the N-ter-

minal six transmembrane domains and are thus predicted to be cytoplasmic and accessible to kinases. Interestingly, prediction of transmembrane topology (Localizome) indicates a seventh transmembrane domain that lies between the FAD and NADPH binding domains. The significance of this is not known. Duox1 and -2 are related enzymes that also possess EF hands and generate ROS in a calcium-dependent manner (1, 18). Comparison of the amino acid sequences of Nox5 and Duox1 and -2 reveals that the region containing the Nox5 phosphorylation sites is absent in Duox1 and -2. The functional significance of this is not yet known. Comparison of the amino acid sequences of the more distantly related Nox2 and Nox4 with Nox5 also confirms that this region is unique to Nox5. Based on the results of the cell-free activity assays, it is clear that the phosphorylation of this region is able to directly increase the sensitivity of Nox5 to calcium. However, it is not yet known whether this modifies the ability of Nox5 to retain bound calcium in an environment of declining calcium concentration and thus maintain the enzyme in an activated state or simply to increase the affinity of the enzyme for calcium.

To our knowledge, the current work is the first demonstration that Nox5 can be activated by PMA. Previous studies have been unable to show that PMA regulates Nox5 activity in human sperm. However, these studies were inconclusive,

Activation of Nox5 via Phosphorylation

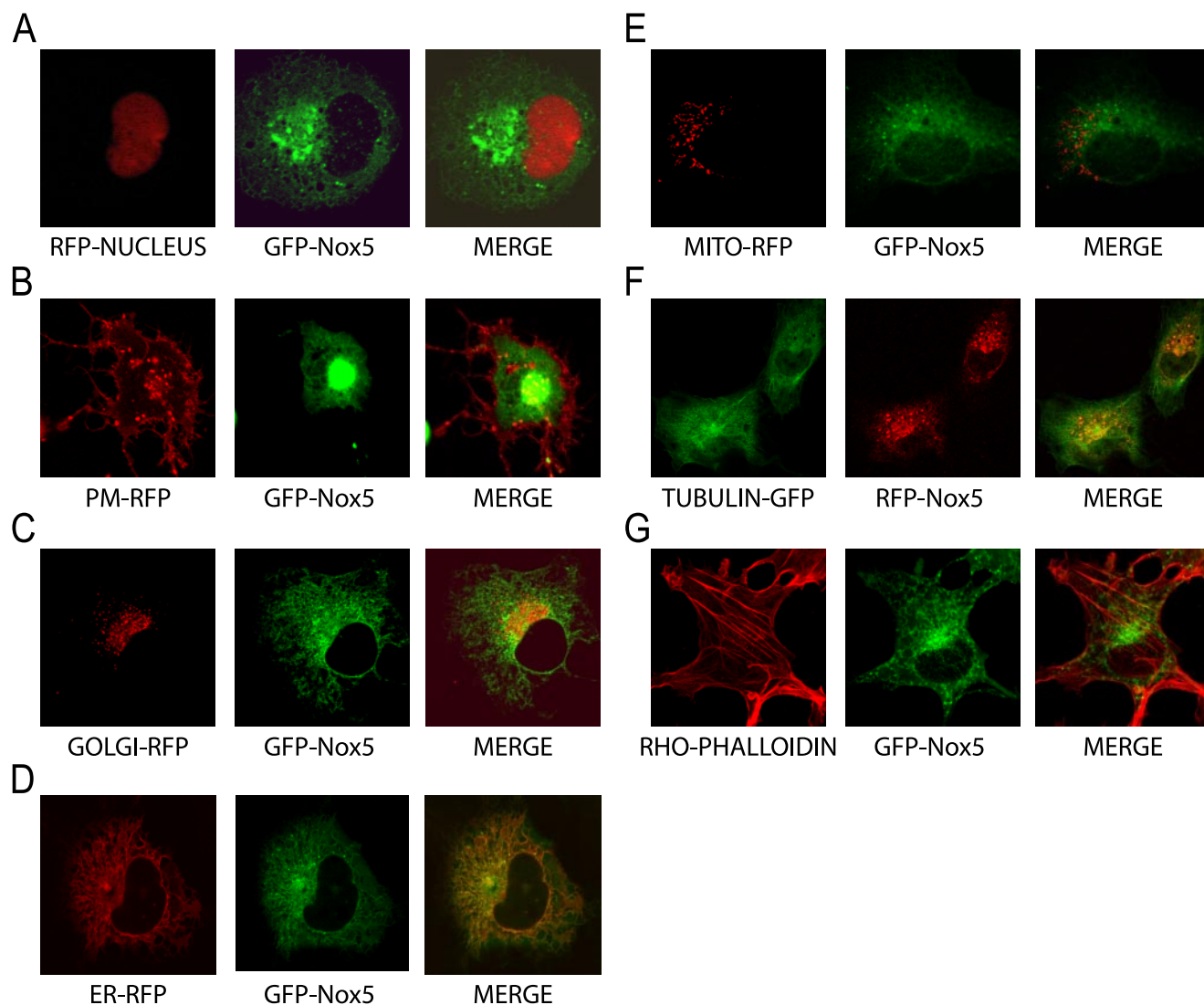


FIGURE 12. **Subcellular location of Nox5 in live cells.** COS-7 cells were transfected with GFP-Nox5 and RFP-NLS (nucleus) (A), GFP-Nox5 and α -1A-RFP (plasma membrane (PM)) (B), GFP-Nox5 and β -1,4-galactosyltransferase-RFP (Golgi) (C), GFP-Nox5 and calreticulin-DSRED (endoplasmic reticulum (ER)) (D), GFP-Nox5 and cytochrome C-RFP (mitochondria) (E), α -tubulin-GFP and RFP-Nox5 (F), or GFP-Nox5 (G). Live cells were visualized for GFP and RFP using confocal microscopy.

since it was not clear whether the cells in question express sufficient Nox5 because very little superoxide production was recorded and there is no indication that the cells actually had the capacity to respond to ionomycin (19). Others have shown that PMA does not regulate the expression level of Nox5 in malignant cells of chronic lymphocytic leukemia and that superoxide production is unaffected by inhibition of protein kinase C with Ro-32-0432 (20). The kinase that phosphorylates Nox5 in response to PMA in the current study is not yet known.

Subcellular fractionation studies revealed that Nox5 is a detergent-insoluble protein that co-fractionates with cytoskeletal proteins. However, this may not represent its true intracellular location, and thus we generated GFP and RFP fusion proteins and visualized the location of Nox5 in live cells using confocal microscopy. These studies revealed that Nox5 is predominantly perinuclear with an extensive network of branching tubules that project into the cytosol. This is a classic distribution of a protein that resides in the endoplasmic reticulum

(21), and indeed there was considerable overlap with the endoplasmic reticulum marker calreticulin but not for other perinuclear proteins, such as the Golgi or mitochondria. In addition, Nox5 was absent from the nucleus and the plasma membrane. The location of Nox5 is similar to that reported for Nox2 and Nox4 (22, 23). The functional significance of Nox5 localization to detergent-insoluble microdomains of the endoplasmic reticulum is not known.

In conclusion, we have shown that PMA facilitates the calcium-dependent activation of Nox5. This occurs through specific phosphorylation of residues 494 and 498 and enhanced enzyme activation at lower and potentially more physiologically relevant concentrations of intracellular calcium.

REFERENCES

1. Lambeth, J. D. (2004) *Nat. Rev. Immunol.* **4**, 181–189
2. Babior, B. M. (2004) *Curr. Opin. Immunol.* **16**, 42–47
3. Sumimoto, H., Miyano, K., and Takeya, R. (2005) *Biochem. Biophys. Res. Commun.* **338**, 677–686
4. Banfi, B., Clark, R. A., Steger, K., and Krause, K. H. (2003) *J. Biol. Chem.*

- 278, 3510–3513
5. Takeya, R., Ueno, N., Kami, K., Taura, M., Kohjima, M., Izaki, T., Nunoi, H., and Sumimoto, H. (2003) *J. Biol. Chem.* **278**, 25234–25246
 6. Cheng, G., Ritsick, D., and Lambeth, J. D. (2004) *J. Biol. Chem.* **279**, 34250–34255
 7. Banfi, B., Malgrange, B., Knisz, J., Steger, K., Dubois-Dauphin, M., and Krause, K. H. (2004) *J. Biol. Chem.* **279**, 46065–46072
 8. Kawahara, T., Ritsick, D., Cheng, G., and Lambeth, J. D. (2005) *J. Biol. Chem.* **280**, 31859–31869
 9. Ambasta, R. K., Kumar, P., Griendling, K. K., Schmidt, H. H., Busse, R., and Brandes, R. P. (2004) *J. Biol. Chem.* **279**, 45935–45941
 10. Banfi, B., Molnar, G., Maturana, A., Steger, K., Hegedus, B., Demaurex, N., and Krause, K. H. (2001) *J. Biol. Chem.* **276**, 37594–37601
 11. Banfi, B., Tirone, F., Durussel, I., Knisz, J., Moskwa, P., Molnar, G. Z., Krause, K. H., and Cox, J. A. (2004) *J. Biol. Chem.* **279**, 18583–18591
 12. Daiber, A., August, M., Baldus, S., Wendt, M., Oelze, M., Sydow, K., Kle-schyov, A. L., and Munzel, T. (2004) *Free Radic. Biol. Med.* **36**, 101–111
 13. Jagnandan, D., Sessa, W. C., and Fulton, D. (2005) *Am. J. Physiol.* **289**, C1024–C1033
 14. Zhang, Q., Church, J. E., Jagnandan, D., Catravas, J. D., Sessa, W. C., and Fulton, D. (2006) *Arterioscler. Thromb. Vasc. Biol.* **26**, 1015–1021
 15. Church, J. E., and Fulton, D. (2006) *J. Biol. Chem.* **281**, 1477–1488
 16. Campbell, R. E., Tour, O., Palmer, A. E., Steinbach, P. A., Baird, G. S., Zacharias, D. A., and Tsien, R. Y. (2002) *Proc. Natl. Acad. Sci. U. S. A.* **99**, 7877–7882
 17. Fulton, D., Gratton, J. P., McCabe, T. J., Fontana, J., Fujio, Y., Walsh, K., Franke, T. F., Papapetropoulos, A., and Sessa, W. C. (1999) *Nature* **399**, 597–601
 18. Ameziane-El-Hassani, R., Morand, S., Boucher, J. L., Frapart, Y. M., Apostolou, D., Agnandji, D., Gnidehou, S., Ohayon, R., Noel-Hudson, M. S., Francon, J., Lalaoui, K., Virion, A., and Dupuy, C. (2005) *J. Biol. Chem.* **280**, 30046–30054
 19. Armstrong, J. S., Bivalacqua, T. J., Chamulitrat, W., Sikka, S., and Hellstrom, W. J. (2002) *Int. J. Androl.* **25**, 223–229
 20. Kamiguti, A. S., Serrander, L., Lin, K., Harris, R. J., Cawley, J. C., Allsup, D. J., Slupsky, J. R., Krause, K. H., and Zuzel, M. (2005) *J. Immunol.* **175**, 8424–8430
 21. Snapp, E. L., Hegde, R. S., Francolini, M., Lombardo, F., Colombo, S., Pedrazzini, E., Borgese, N., and Lippincott-Schwartz, J. (2003) *J. Cell Biol.* **163**, 257–269
 22. Van Buul, J. D., Fernandez-Borja, M., Anthony, E. C., and Hordijk, P. L. (2005) *Antioxid. Redox. Signal.* **7**, 308–317
 23. Bayraktutan, U., Blayney, L., and Shah, A. M. (2000) *Arterioscler. Thromb. Vasc. Biol.* **20**, 1903–1911